Eur. Phys. J. A **20**, 419–427 (2004)
DOI 10.1140/epja/i2003-10159-2

THE EUROPEAN PHYSICAL JOURNAL A

# Experimental puzzle of $^5$H

L.V. Grigorenko[a]

GSI, Planckstrasse 1, D-64291, Darmstadt, Germany and Russian Research Center "The Kurchatov Institute", 123182 Moscow, Russia

Received: 22 April 2003 / Revised version: 8 November 2003 /
Published online: 18 June 2004 – 
Communicated by G. Orlandini

**Abstract.** The experimental evidences for $^5$H are discussed. The results of the recent experiments are controversial. We make a comparison of the experimental data with theoretical calculations (L.V. Grigorenko, N.K. Timofeyuk, M.V. Zhukov, Eur. Phys. J. A **19**, 181 (2004)) and try to find a consistent explanation for the current experimental situation. We conclude that more detailed experimental information is required to resolve the existing experimental ambiguity.

**PACS.** 21.45.+v Few-body systems – 21.60.Gx Cluster models – 25.10.+s Nuclear reactions involving few-nucleon systems

## 1 Introduction

In paper [1] we have addressed some general and qualitative questions of treatment of the broad few-body states. We have found that the broad structures in the few-particle continuum could have quite a specific nature and qualitatively different dynamics in comparison with ordinary nuclear states. They could be caused, for example, by slow motion in the internal region and tunneling between multiple channels, rather than reflection from some potential barrier. It was shown that for broad few-body states all the three ingredients of reaction theory become important: i) initial structure, ii) reaction mechanism, and iii) final-state interaction (FSI).

Studies in paper [1] were carried out mainly on the example of $^5$H. They were, actually, inspired by the recent revival of interest to this system, both experimental [2–4] and theoretical [5–8]. The experimental situation appears to be extremely complicated, so this paper is dedicated solely to the discussion of experiments and attempts to understand their relation with theoretical predictions [1].

There is also some methodological issue which is relevant to many experiments studying the states with multiparticle decay channels. For broad states the experimentalists are ordinarily testing the data for deviation from phase volume. This is not always done in a formally correct way. For example, the final-state interaction amplitudes may sometimes be used, which do not take into account Pauli principle for the decay products properly. The use of the hyperspherical decomposition of amplitudes for decay products allows to avoid this problem and makes a connection with theoretical calculations quite straightforward.

**Table 1.** The experimental results on $^5$H ground-state energy and width (given in MeV). $E_{\rm T}$ is the energy relative to the $t+n+n$ threshold.

| Paper | $E_{\rm T}$ | $\Gamma$ | Method |
|---|---|---|---|
| Adelberger [9] | $> 2.1$ | | $^3$He($^3$He, $n$)$^5$Be |
| Young [10] | 2.15 | 1.5 | $^3$H($t$, $p$)$^5$H |
| Gornov [13,14] | 7.4(7) | 8 | $^9$Be($\pi^-$, $pt$ or $dd$)$^5$H |
| Aleksandrov [16] | 5.2(4) | 4 | $^7$Li($^6$Li, $^8$B)$^5$H |
| Korsheninnikov [2] | 1.7(3) | 1.9(4) | $p$($^6$He, $2p$)$^5$H |
| Gornov [18] | 5.5(2) | 5.4(5) | $^9$Be($\pi^-$, $pt$ or $dd$)$^5$H |
| Golovkov [3] | 1.8(1) | $< 0.5$ | $^3$H(t, $p$)$^5$H |
| Meister [4] | 3 | 6 | $^{12}$C($^6$He, $^5$H)X |

The results of conclusive experiments [9–16,2–4] concerning $^5$H are listed in the table 1. There is also a number of experiments, where $^5$H has not been observed. In the others the authors are cautious about their results and claim a low confidence level. A lower limit on the mass of $^5$H was obtained in [9] from the absence of sharp structures in the "mirror" $^3$He($^3$He, $n$)$^5$Be reaction up to 4.2 MeV. This implies that $^5$H is unbound by at least 2.1 MeV. According to [15] nothing except the phase space, modified by dineutron decay was found in the pion absorption reactions $^6$Li($\pi^-$, $p$)$^5$H. The point of view of [15] on their data was opposed in [17,6]. It was demonstrated in [17] that the spectrum in [15] allows different interpretations including one with a state in $^5$H. It was found in [6] that "dineutron" emission, if considered correctly, should lead

[a] e-mail: L.Grigorenko@gsi.de

to a significantly smaller impact on the phase volume than was estimated in [15]. A $^5$H state candidate with a resonance energy $E_{\rm T} = 7.4 \pm 0.7$ MeV, $\Gamma = 8 \pm 3$ MeV was detected in the $^9$Be$(\pi^-, pt)^5$H reaction [13,14]. The new measurement of the same reaction (with better resolution and statistics) gives peaks at 5, 10, 18, and 26 MeV [18]. In the $^7$Li($^6$Li, $^8$B)$^5$H reaction [16] a resonance at about $E_{\rm T} = 5.2$ MeV, $\Gamma = 4$ MeV was observed. Sharp peaks corresponding to the ground state of $^5$H were observed in $p(^6$He, $2p)^5$H [2] and $^3$H$(t, p)^5$H [3] reactions at the energies $E_{\rm T} = 1.7 \pm 0.3$ and $E_{\rm T} = 1.8 \pm 0.1$ MeV. These results agree reasonably with each other. The high-energy experiment $^{12}$C($^6$He, $^5$H)X [4] shows only a broad peak at about 3 MeV. A detailed discussion of the recent experiments is provided below in this paper.

## 2 Discussion of the $^6$He(p, 2p) reaction at 36 MeV/u

The experiment [2] was a missing-mass measurement, where the role of the recoil particle was played by two protons measured in coincidence. The empty histogram in fig. 1 shows the $^5$H spectrum [2] measured in coincidence with the triton from the decay of the residual $^5$H system (to eliminate the background from the empty target measurement). The authors investigated carefully various kinds of the $t+n+n$ continuum and came to the conclusion that the upper part of the spectrum could be attributed to different processes, where the full $t + n + n$ final-state interaction is not incorporated. Consequently, the authors of [2] interpreted the 2 MeV peak in the spectrum as a state in $^5$H. Fitting the total spectrum they got for the $^5$H state a resonance energy $E_{\rm T} = 1.7 \pm 0.3$ MeV and a width $\Gamma = 1.9 \pm 0.4$ MeV. There is another essential piece of information in ref. [2]. Namely, the energy distribution between protons and the angular distribution of the "diproton" have been deduced from the data. These distributions give evidence that the transferred angular momentum in the reaction is zero. So, we can expect that the low-energy peak corresponds to the $1/2^+$ ground state of $^5$H.

We would like to apply our "model with source" approach (MWS, see sect. 3 of ref. [1]) for the description of this experiment. However, before we apply the MWS a few words of precaution are needed. In the derivation of the source, which is one of the main ingredients of our model, we assume a sudden removal of a proton from the alpha core in $^6$He. In the experiment [2] the incident $^6$He energy is not very large (giving about 10 MeV energy above the $(t+2n+2p)$ threshold in the center of mass). So, MWS, if applicable at all, should be applied only to the low-lying part of the spectrum in fig. 1, where the "diproton" c.m. is moving with relatively large velocity relative to the $^5$H c.m. In this section we consider only the part of the spectrum, which corresponds in the framework of the MWS to the $1/2^+$ ground-state $^5$H system.

We can see in fig. 1 that the experimental peak position is much lower than the "usual" 3.2–3.5 MeV obtained with a full $^6$He WF source in MWS (solid curve). There can be

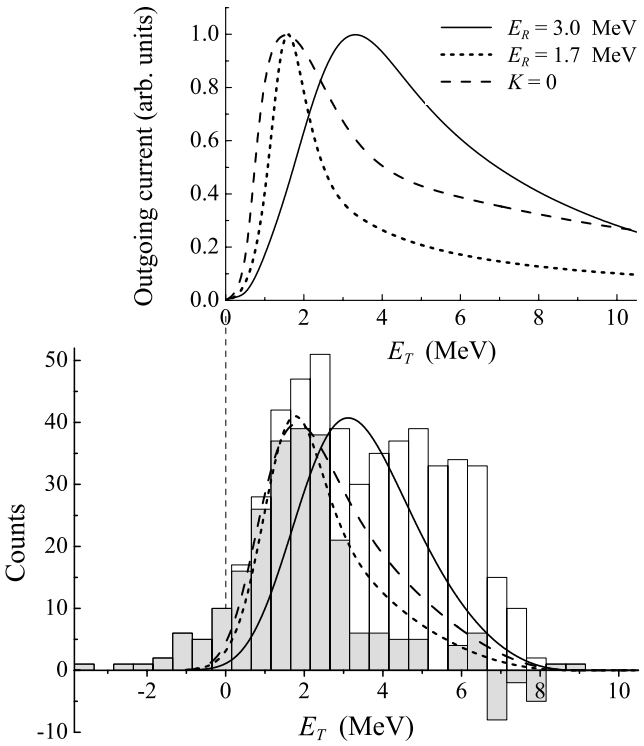


**Fig. 1.** The experimental data taken from ref. [2] are shown by the empty histogram. The gray histogram shows the same, but with some smooth subtraction of the high-energy contribution (there could be different versions of such subtraction; it is shown only for convenience). The solid and dashed curves show the full MWS calculation and $K = 0$ in the source (the same curves as in fig. 3a in [1]). The dotted curve is obtained with a full $^6$He source but the system is artificially bound by a three-body force. In the upper plot the theoretical curves are shown. In the lower plot they are given after convolution with experimental resolution, efficiency, and energy cut-offs.

two explanations for this situation connected with $^5$H itself and with the observation conditions: i) In reality the $^5$H ground state is more bound than what we can obtain in a cluster model. ii) Our structure model is adequate, but the reaction mechanism shifts the peak to a lower energy. The options i) and ii) can be distinguished experimentally, as they provide, according to our calculations [1], different correlation spectra (see fig. 4 in [1]). No such information is available in experiment [2].

For scenario i) there can be two reasons:

a) The cluster model is adequate, but the interaction in the $t$-$n$ channel is actually more attractive than what was used in refs. [19,20,6]. This can easily be checked. To provide the 1.8 MeV ground state in $^5$H we need to have a ground state in the $^4$H subsystem at 1.4–1.8 MeV, which is lower than the typical experimental values around 2.5–3.2 MeV. At the same time note, however, that in [4] $^4$H has energy 1.6 MeV.

b) There is an extra attraction in the system, and its reason is beyond the cluster model (say, 5-nucleon effect). It is well known that the $^6$He nucleus in the three-cluster

models with $\alpha$-$n$ interactions fitted to experimental data is underbound by about 700 keV. Somewhat stronger potentials in this channel are used to get the experimental binding of $^6$He ([21] and references therein). We can use a phenomenological attractive three-body potential (see eq. (10) in [1]) to lower the peak position in the $^5$H spectrum (dotted curve in fig. 1).

For scenario ii), again, two situations should be distinguished:

a) It was shown in [1] that a selective population of components of the $^5$H WF can lead to strong variations in the spectrum (see fig. 4a in [1]). Calculations without *any modification of interactions*, but with a population of the $K = 0$ component in $^5$H only are consistent with the experimental spectrum observed in [2] (dashed curve in fig. 1).

b) The spectrum of $^5$H can be modified by interaction with recoil particles. This possibility is the most unpleasant situation and it is discussed separately below.

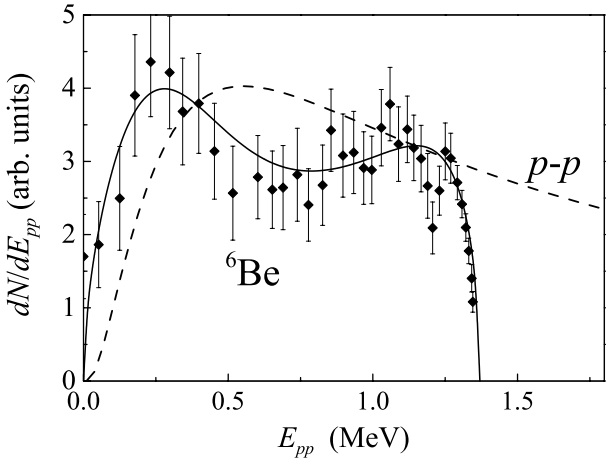


**Fig. 2.** Spectrum of proton-proton relative motion. Experimental data: missing-mass spectrum of two protons from the decay of the $^6$Be g.s. [26]. The solid curve shows three-body decay calculations [33]. The dashed curve is the proton-proton $s$-wave scattering cross-section.

### 2.1 Spectrum modification due to interaction with recoil particles

Careful studies have been performed in [2] to assure that the 1.7 MeV peak in the spectrum cannot be connected with pairwise FSI in the subsystems or with known states in $^5$He and $^5$Li. More complicated reasons, however, cannot be excluded by such an analysis. The total c.m. energy available for 5 particles ($2p$, $2n$, and $t$) is about 10 MeV in the reaction [2]. This means that for $^5$H events, stemming from the $E_{\rm T} = 1.7$ MeV peak, the neutrons have on average about 1 MeV energy, while protons have on average about 4 MeV. For a relative energy of 4 MeV between triton and proton the states in the $\alpha$-particle (broad $1^-$ and tail of broad $2^-$) can be populated. At this energy the protons spend only twice less time in the interaction region than the neutrons. For these reasons the internal motion of $^5$H cannot be expected to be well factorised from the motion of the recoil $2p$ system (see the discussion of possible model approximations in appendix B of ref. [1]). In this situation we cannot exclude that the shape of the spectrum is strongly influenced by the simultaneous combination of pairwise interactions (say, 5-body FSI: $t+2n+2p$), not just by one of them or only by a selected set of FSIs (say, only those which form $^5$H).

Theoretical calculations of such effects are beyond our abilities. We can only illustrate this point qualitatively by analogy with the experimentally studied and theoretically well-understood situation in the decay of the $^6$Be g.s. If we attempt to study the FSI between two protons in this decay, there is a problem. The peak that can be associated with a "diproton" can be found in the missing-mass spectrum of the "diproton" (reconstructed from the $\alpha$-particles) at an energy twice lower than the maximum in the "bare diproton" (as given by the proton-proton cross-section). One can interpret this result as follows: the interaction with the recoil particle (the $\alpha$-particle in this experiment), under the condition of small total energy available to all particles, leads to a significant lowering of the peak in the missing-mass spectrum of the unstable system ($p$-$p$ in this reaction). Another interpretation is that this spectrum reflects the structure of the $^6$Be g.s., which is dominated by $p$-waves, which, together with the Pauli principle, are responsible for the double-hump structure in the spectrum shown in fig. 2. Whatever the interpretation is, in fact this spectrum does not provide straightforwardly the information about the decay properties of the $p$-$p$ system.

The analogy of the $^6$Be case with the experiment from ref. [2] is supported by similar energy conditions: $E_{^5{\rm H}}/E_{^5{\rm H}+2p} = 0.17$ and $E_{pp}/E_{pp+\alpha} = 0.19$. However, there is some argument against such interpretation: the energy spectrum of the diproton (which is a recoil particle in this experiment) is not modified compared to the "bare diproton" ($p$-$p$ scattering). Anyhow, a possibility of the spectrum modifications induced by interactions with the recoil cannot be entirely proven or disproved by speculations. In any low-energy experiment such possibility in principle exists. It can, however, be rejected experimentally if the same experiment is performed at different energies and the peak position remains at the same place.

## 3 Discussion of the $^6$He($^{12}$C,$^5$H)X reaction at 240 MeV/u

The high-energy experiment [4] is well suited for comparison with the MWS reaction model. In this experiment all the fragments from the $^5$H system after proton removal from $^6$He were registered in coincidence and the full kinematics of the reaction was reconstructed. The average momentum transfer to the $^5$H center of mass in this reaction was below 40 MeV/$c$, which means that an approximation, in which the source function can be represented in the factorised form (see eq. (26) in [1]) works well. The efficiency corrected invariant-mass spectrum from this experiment

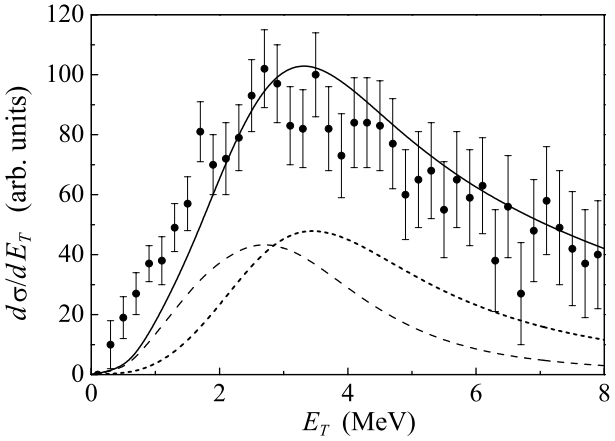


**Fig. 3.** Invariant-mass spectrum of $^5$H from [4]. The solid curve corresponds to the full MWS calculation (it is the same as the solid curve in fig. 1). The dashed and dotted curves show the partial contributions of components with amplitudes $A_{000}^{01/20}$ and $A_{000}^{21/20}$ (see text).

is shown in fig. 3 together with the MWS calculation. The spectrum shows a broad peak at about 3 MeV. The agreement with the MWS calculation is good.

### 3.1 Three-body momentum distributions

The availability of full kinematics data with large acceptance makes possible to recover the full momentum correlations. For three (and more) products in the final state the differential cross-section can be expanded on a set of hyperspherical amplitudes. This kind of experimental data analysis was suggested in [22] and was realized for the first time in [23]. The method was used in the analysis of the experimental results for decays of narrow $^6$Be $0^+$, $^6$Be $2^+$, $^6$He $2^+$ states [24–29] and $^9$Be $5/2^-$, $^9$B $5/2^-$ states [30].

The cross-section depends on the Jacobi momenta $\mathbf{k}_x$ and $\mathbf{k}_y$ conjugated to Jacobi vectors (see fig. 13 in [1]). In the coordinate system, where the axis $z$ is collinear with the vector $\mathbf{k}_y$ and after summation over unobservable spin variables the cross-section can be written as a function of three variables: the total energy $E_{\rm T}$, the energy distribution $\varepsilon = E_x/E_{\rm T} = \sin^2\theta_\kappa$ between subsystems, and the angle $c_k = \cos\theta$ between vectors $\mathbf{k}_x$ and $\mathbf{k}_y$. Using eqs. (6), (7), and (15) from [1] we get

$$\frac{\mathrm{d}^3 j}{\mathrm{d}E_{\rm T}\,\mathrm{d}\varepsilon\,\mathrm{d}c_k} = \sqrt{\frac{2E_{\rm T}}{M}}\sqrt{\varepsilon(1-\varepsilon)}\sum_{LSS_x}\sum_{KK'}\sum_{l_x l'_x l_y l'_y} \times \left(A^{K'SS_x}_{Ll'_x l'_y}(E_{\rm T})\right)^* A^{KSS_x}_{Ll_x l_y}(E_{\rm T})\,\psi^{l'_x l'_y}_{K'}(\theta_\kappa)\psi^{l_x l_y}_{K}(\theta_\kappa) \times \frac{\hat{l}'_y \hat{l}_y}{2L+1}\sum_m C^{Lm}_{l'_x m l'_y 0} C^{Lm}_{l_x m l_y 0}\, N^m_{l'_x} P^m_{l'_x}(c_k)\, N^m_{l_x} P^m_{l_x}(c_k)\,, \quad (1)$$

where $j$ is the current through the hypersphere of large radius (which is proportional to the cross-section) and $N^m_{l_x} P^m_{l_x}(c_k)$ are the Legendre polynomials normalized to unity. The detailed discussion of the three-body correlations with application to two-proton radioactivity can also be found in [31].

**Table 2.** Parametrization of the measured momentum distribution for $^5$H in the "T" Jacobi system [4]. The total probability is normalized to unity. The same values for the calculated distributions are given in column "Th.". The relative internal normalization of the corresponding components of the WFs for $^5$H and $^6$He are given in columns $N(^5\mathrm{H})$ and $N(^6\mathrm{He})$.

| Parameter | Exp. | Th. | $N(^5\mathrm{H})$ | $N(^6\mathrm{He})$ |
|---|---|---|---|---|
| $\lvert\overline{A}^{0S0}_{000}\rvert^2$ | 0.18(3) | 0.360 | 0.154 | 0.041 |
| $\lvert\overline{A}^{2S0}_{000}\rvert^2$ | 0.45(2) | 0.430 | 0.652 | 0.773 |
| $\lvert\overline{A}^{2S1}_{111}\rvert^2$ | 0.37(4) | 0.111 | 0.116 | 0.146 |
| $\overline{A}^{2S0}_{000}\overline{A}^{0S0}_{000}/\lvert\overline{A}^{2S0}_{000}\rvert\,\lvert\overline{A}^{0S0}_{000}\rvert$ | 0.48(3) | 0.976 | | |

The spectra of the particles cannot be used straightforwardly for comparison with theory due to complicated corrections for experimental setup efficiency. In paper [4] the experimental data in the interval 1–5 MeV were fitted with a minimal set of three-body decay amplitudes, using a procedure taking into account the properties of the experimental setup. Due to comparatively low statistics the correlation functions had to be averaged over the energy:

$$W(\varepsilon, c_k) = \int_1^5 \mathrm{d}E_{\rm T}\frac{\mathrm{d}^3 j}{\mathrm{d}E_{\rm T}\,\mathrm{d}\varepsilon\,\mathrm{d}c_k}\,.$$

Under the assumption that all the amplitudes have the same energy dependence (and correspondingly phases are energy independent) the integrated correlation density function $W(\varepsilon, c_k)$ can be expressed via amplitudes $\overline{A}$, averaged over the energy interval: $\overline{A}^{KSS_x}_{Ll_x l_y} = \langle A^{KSS_x}_{Ll_x l_y}(E_{\rm T})\rangle_{E_{\rm T}}$. It should be understood, however, that the amplitudes found in theoretical calculations have different dependences on energy and these differences are not negligible (see, for example, dashed and dotted curves in fig. 3).

It was found in [4] that a set of four lowest hyperspherical amplitudes $A^{KSS_x}_{Ll_x l_y}$ can reproduce the experimental momentum distribution with $\chi^2$ below unity.

$$W(\varepsilon, c_k) = \frac{4}{\pi}\sqrt{\varepsilon(1-\varepsilon)}\left[8\varepsilon(1-\varepsilon)(1-c_k^2)\left|\overline{A}^{2S1}_{111}\right|^2 + \left|\overline{A}^{0S0}_{000} - 2(2\varepsilon-1)\overline{A}^{2S0}_{000} - 4\sqrt{\varepsilon(1-\varepsilon)}c_k\overline{A}^{2S0}_{011}\right|^2\right]. \quad (2)$$

Only the component with total spin $S = 1/2$ is required for the fit. The amplitudes $A^{0S0}_{000}$ and $A^{2S1}_{111}$ are the same both in the "T" and "Y" coordinate systems. The amplitude $A^{2S0}_{011}$ should be zero in the "T" Jacobi system due to the Pauli principle between two neutrons. This leads to condition

$$A^{2S0}_{011}/A^{2S0}_{000} = -0.96825/0.25$$

in the "Y" Jacobi system according to Raynal-Revai coefficients. This leaves us with four real independent coefficients in experimental fit, which are listed in table 2.

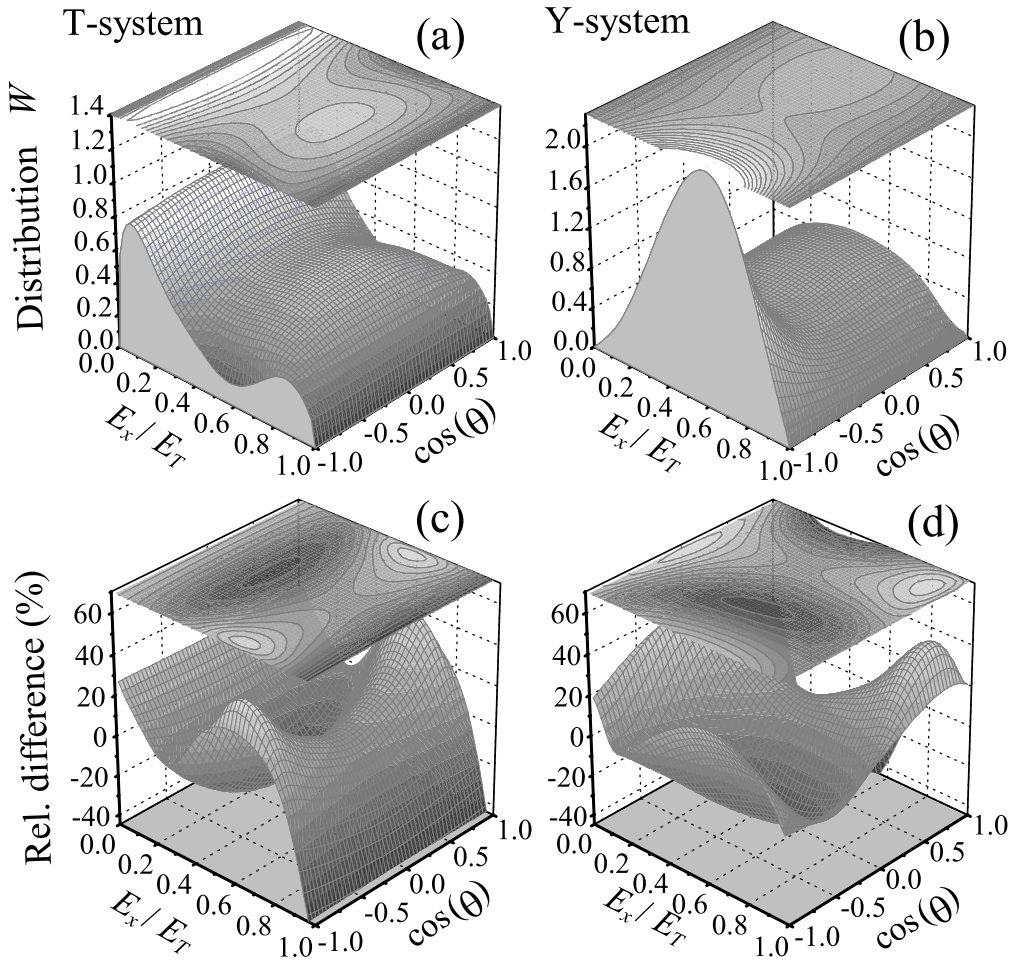


**Fig. 4.** Momentum distributions calculated for the $^5$H $1/2^+$ state (integrated in the range $1 < E_{\rm T} < 5$ MeV, see fig. 3) in the "T" (a) and "Y" (b) Jacobi systems. Relative differences between calculated and fitted distributions taken from ref. [4] are given in the "T" (c) and "Y" (d) Jacobi systems.

In fig. 4 the correlation functions (calculated for the solid curve in fig. 3) are shown in the $\{\varepsilon, c_k\}$-plane both in the "T" and "Y" Jacobi coordinate systems. The spectra projected on the $\varepsilon$ and $c_k$ axis are shown in fig. 5. Because it is visually difficult to find much difference with the fitted experimental distribution eq. (2) we show in the second row of fig. 4 the relative difference between theoretical and experimental distributions $(W_{\rm th} - W_{\rm exp})/W_{\rm th}$. The observed deviations are generally rather small: they are mostly below 25% and only in some places they exceed 50%. Such agreement is quite interesting considering the simple reaction model used and the quite large uncertainties in the experimental data.

### 3.2 Qualitative features of the correlations

The distributions show the following main features. There is a strong evidence for a $n$-$n$ final-state interaction both in "T" and "Y" systems. In "T" system the energy distribution has a broad peak at small energy between neutrons (fig. 4(a)). In the "Y" system this corresponds to a peak at angle $\theta$ about $\pi$ (fig. 4(b)), which means that momenta of neutrons are practically colinear. The energy distribution between two neutrons also has a broad component which reflects the initial structure of $^6$He dominated by $K = 2$. The first example of such broad distribution was obtained in [24,26] for the decay of the $^6$Be ground state and characterized as "democratic decay".

The projected energy distribution between $n$ and $t$ fig. 5(a) is quite broad and symmetric. Still its shape is clearly distinguishable from phase volume $\sqrt{\varepsilon(1-\varepsilon)}$ and is quite close to the shape expected for $p$-wave emission $(\varepsilon(1-\varepsilon))^{3/2}$. It is interesting to note that small asymmetry, shifting the peak position to higher $n$-$t$ energies is connected with the small mass of the core. This can be illustrated by the simple limiting case: if we assume zero energy between two neutrons ($E_x = 0$ in the "T" system) then the energy between core and neutron ($E_x$ in the "Y" system) is

$$E_x = \frac{E_{\rm T}}{2}\frac{A_c+2}{A_c+1} = 0.625 E_{\rm T}\,. \qquad (3)$$

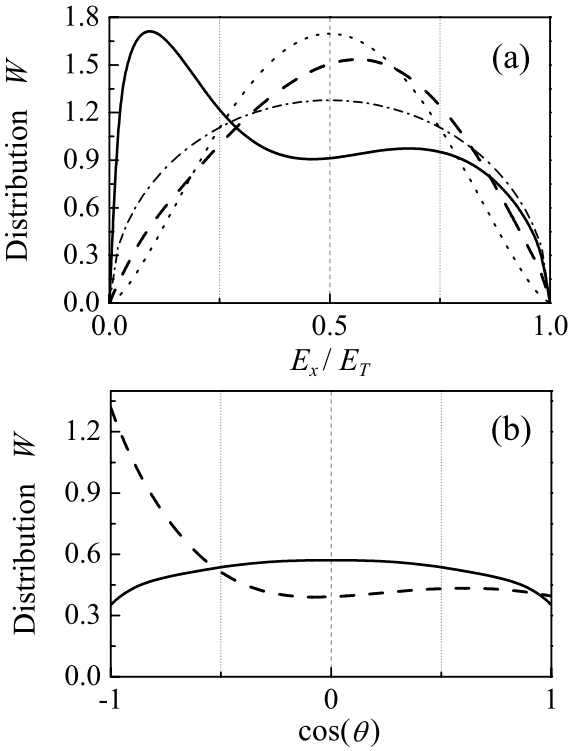


**Fig. 5.** Projections of the distributions of fig. 4 on the $E_x/E_{\rm T}$ and the $\cos(\theta)$ axis. Solid curves are for "T" and dashed curves are for "Y" Jacobi systems. Phase space (dash-dotted curve) and $p$-wave emission (dotted curve) are depicted in (a) for comparison.

The energy distribution fig. 5(a) in the "T" system has a strong peak at low $n$-$n$ energy, so the maximum in the distribution in the "Y" system is shifted to $\varepsilon = 0.57$. Core-$N$ distributions calculated for decays of heavier systems (two-proton emitters [32,33]) show a very high degree of symmetry.

One can see from table 2 that the calculated lowest amplitudes differ strongly from the corresponding ones fitted to the experimental data. If we use only these theoretical amplitudes, the obtained distribution will be strongly different from the measured one. However, the total calculated distribution has a very high identity with the fitted one. This is due to 10% contribution of higher amplitudes (not shown in the table) in the distribution. This means that the physics underlying the measured distribution is different from the one deduced from experiment using the assumption that the FSI does not modify the weights of components significantly. If we consider the fitted amplitudes, we see a strong enhancement of the $S_x = 1$ configuration compared to the initial $^6$He WF. Such enhancement has no qualitative explanation in a simple reaction mechanism, ordinarily assumed for such a reaction. If we look at the evolution of the calculated values in table 2 (normalization of components in $^6\mathrm{He} \rightarrow$ internal normalizations in $^5\mathrm{H} \rightarrow$ decay amplitudes in $^5$H), then it is quite natural: the $S_x = 1$ component is stable, but there is a strong change of the $K = 0$ component. The $K = 0$ component is quite suppressed in $^6$He due to Pauli principle. It is larger "inside" $^5$H as it is a more diluted system, and asymptotically the $K = 0$ amplitude contributes more than one third to the total decay probability.

The calculated dependence on the angle $\theta$ in the "T" system has on average shape close to

$$W \sim 1 - C_2 \cos^2(\theta)\,, \tag{4}$$

see fig. 5(b). In the fitting procedure this results in a large contribution of the $S_x = 1$ component. This component is the only in the fit which has the required dependence on $\theta$ (see eq. (2)). In calculations this dependence has a different physical origin as the $S_x = 1$ component is quite small. The coefficient $C_2$ has a strong dependence on the energy between the neutrons. This can be seen in fig. 4(a). There is a minimum at $\varepsilon \sim 0.55$–$0.65$. It is easy to find out that at angles $\theta = 0$ and $\theta = \pi$ (one of the neutrons is flying out in the same direction as the triton) neutron and triton will have the same velocities as the energy between neutrons is given by eq. (3) to be $\varepsilon = 0.625$ (but now in the "T" system). At small relative momentum neutron and triton should "feel" only mutual repulsion due to Pauli principle. So, in the calculations the dependence of eq. (4) comes mainly as a result of the dynamic treatment of Pauli repulsion in the $t$-$n$ channel and only partly as a result of the population of the $S_x = 1$ component which naturally has such dependence.

### 3.3 Possibility of the alternative interpretation

Good agreement between theory and experiment is found above not only for inclusive characteristics (invariant-mass spectrum) but also for highly detailed particle correlation data. It seems that we have a good understanding, both qualitative and quantitative, of all features of correlation spectra. However, it should be understood that the given analysis of the experimental data does not exclude a completely alternative interpretation of the data.

Let us look on the correlation function for excited states of $^5$H:

$$\begin{aligned} W(\varepsilon, c_k) = \frac{32}{5\pi}\sqrt{\varepsilon(1-\varepsilon)}\Big\{ & 2\varepsilon^2 \left|\overline{A}^{2S0}_{220}\right|^2 + 2(1-\varepsilon)^2 \left|\overline{A}^{2S0}_{202}\right|^2 \\ & + \varepsilon(1-\varepsilon)(3+c_k^2)\left|\overline{A}^{2S0}_{211}\right|^2 + 5\varepsilon(1-\varepsilon)(1-c_k^2)\left|\overline{A}^{2S1}_{111}\right|^2 \\ & + 4\sqrt{2\varepsilon(1-\varepsilon)}c_k\,\mathrm{Re}\left[\left(\varepsilon\overline{A}^{2S0}_{220} + (1-\varepsilon)\overline{A}^{2S0}_{202}\right)\overline{A}^{2S0}_{211}\right] \\ & + 2\varepsilon(1-\varepsilon)(3c_k^2-1)\,\mathrm{Re}\left[\overline{A}^{2S0}_{202}\overline{A}^{2S0}_{220}\right]\Big\}\,, \end{aligned} \tag{5}$$

where $S = 1/2$ is assumed. As far as this function is obtained by spin averaging, it is the same both for $5/2^+$ and $3/2^+$ excited states of $^5$H. The basis truncation here is the same as in formula (2), so the fits are expected to have the same quality. Again, as in the case of the $1/2^+$ state, the Pauli principle excludes the amplitude $A^{2S0}_{211}$ in the "T" system and the amplitude $A^{2S1}_{211}$ is the same in the

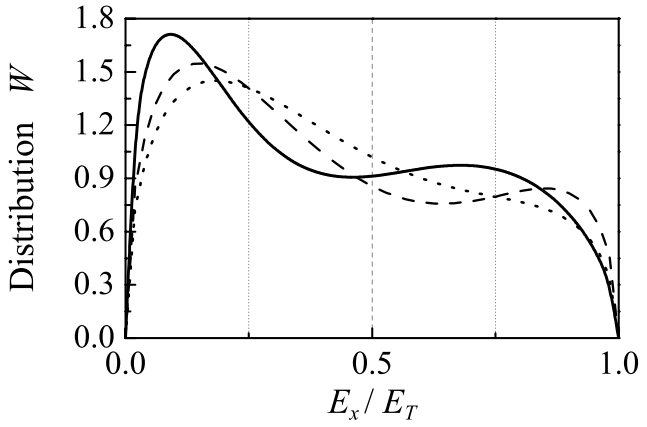


**Fig. 6.** Projected distributions in the "T" system ($E_x$ is the energy between neutrons). Comparison of calculations for $1/2^+$ (solid curve; the same as in fig. 5(a)), experimental fit assuming $1/2^+$ (dashed curve), experimental fit assuming $5/2^+$ (dotted curve).

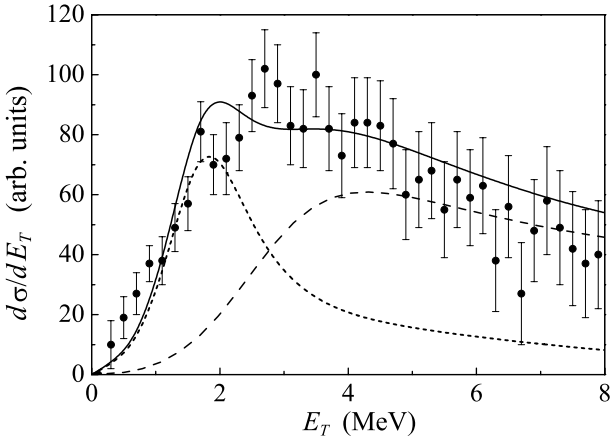


**Fig. 7.** Invariant-mass spectrum of $^5$H from [4]. The dotted curve is the same as in fig. 3. The dashed curve is the contribution from the $5/2^+$ and $3/2^+$ states of $^5$H multiplied by an arbitrary coefficient. The solid curve is a sum of the three low-lying states.

"T" and "Y" systems. The rules for transformation of the amplitudes to "Y" system are:

$$A^{2S0}_{220} = 0.375\, A^{2S0}_{220} + 0.625\, A^{2S0}_{202}$$
$$A^{2S0}_{202} = 0.625\, A^{2S0}_{220} + 0.375\, A^{2S0}_{202}$$
$$A^{2S0}_{211} = 0.68465\left(A^{2S0}_{202} - A^{2S0}_{220}\right) .$$

With coefficients $|A^{2S0}_{220}|^2 = 0.325$, $|A^{2S0}_{202}|^2 = 0.672$, $|A^{2S1}_{211}|^2 = 0.003$, $\overline{A}^{2S0}_{220}\overline{A}^{2S0}_{202}/|\overline{A}^{2S0}_{220}|\,|\overline{A}^{2S0}_{202}| = -0.65$ we can obtain a fit, which is quite close to the fit assuming $1/2^+$ state. The maximal difference between these fits can be found for relative energy distribution in the "T" system (see dashed and dotted curves in fig. 6). It is actually not very significant considering statistics in this experiment.

If the ground state of $^5$H is in reality located at about 2 MeV, then we can expect excited states to be at about 4 MeV ($5/2^+$) and 6 MeV ($3/2^+$). This comes out if we scale the spectrum obtained in [6]. In such case it may happen that the invariant-mass spectrum [4] is significantly influenced by excited states of $^5$H. How this situation may look like is shown in fig. 7. The dotted curve shows the $1/2^+$ state contribution consistent with the results of [2]. Contributions of excited states given in this figure are also artificially shifted towards lower energies. We have to enhance them also several times, as model [1] predicts smaller population of excited configurations than required for such interpretation. In experiment [2] the spectrum of the recoil "diproton" particle was shown to be consistent with transferred angular momentum $\Delta l = 0$. For the knockout reaction of [4] we also expect $\Delta l = 0$, but on the basis of the available data, we cannot exclude $\Delta l = 2$. This possibility for the interpretation is shown in fig. 7. To be confident about $\Delta l = 0$, the momentum distribution of the $^5$H center of mass should be studied.

We see that both theory and analysis of experiment [4] favour the ground $1/2^+$ state at about 3 MeV, but an interpretation consistent with experiment [2] (ground state at about 1.7 MeV) cannot be completely excluded by these results.

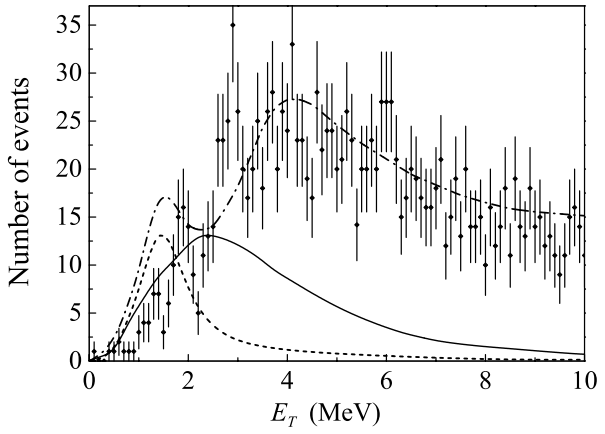


**Fig. 8.** Invariant-mass spectrum of $^5$H from [3]. The solid and dotted curves are the same calculations as in fig. 1, but corrected for experimental efficiency. The dash-dotted curve is the sum of the dotted curve and possible contributions of other than $^5$H population reaction mechanisms as they are given in ref. [3].

## 4 Discussion of t(t, p) reaction at 57 MeV

The missing-mass spectrum of $^5$H from [3] can be found in fig. 8. This spectrum features a broad bump at 3–4 MeV and narrow peaks at 1.8 MeV and 2.7 MeV (much less reliable) whose signatures have quite a low statistical confidence. The widths of the narrow peaks (less than 0.5 MeV) are comparable with instrumental resolution in this experiment, so underlying structures should be even more narrow.

One can see in fig. 8 that calculations which are consistent with experiments [4] (solid curve) or [2] (dotted curve) after experimental efficiency is taken into account produce peaks at different energies. The widths of the theoretical peaks are also too large to match the experimental widths even without any experimental resolution taken into account. It means that if such narrow structures really exist they are beyond the cluster model we use.

Significant difference of experiment [3] from experiments [2,4] is that it is a transfer reaction, not a proton removal. This mechanism does not suggest much selectivity in the sense of transferred angular momentum. It is possible that the ground-state population is hindered in this mechanism. A simple idea about such hindrance is given by angular-momentum combinatorial factors, which give

$$[(2 \cdot 5/2 + 1) + (2 \cdot 3/2 + 1)] / (2 \cdot 1/2 + 1) = 5$$

times more feeding to excited states $5/2^+$ and $3/2^+$ states of $^5$H. It is clear from fig. 8 that these excited states should be essential for the interpretation of this experiment.

No correlation spectra are available for the peaks in [3] due to low statistics and problems with quasi-free scattering. So, no more detailed studies can be carried out here. Studies with better statistics are clearly required to reject or to confirm 1.8 MeV and 2.7 MeV peaks.

## 5 Conclusion

The interpretation of the current experimental situation is complicated. It is very difficult to find a non-contradictory scenario for all experimental data. One possible explanation is that the $^5$H ground state is located at 1.7 MeV, excited states at 4–6 MeV and that in experiment [4] mainly excited states are populated. In that case our theoretical model requires that extra binding is added. The other possibility is that the ground state of $^5$H is at about 3 MeV, as predicted by theory, but for low-energy experiment [2] the peak position is modified. Such modification can be due to selectivity of the reaction mechanism (as was shown in [1]) or because of a non-negligible interaction with recoil particles. The existing experimental evidence does not allow to exclude completely either of these scenarios.

We find the current situation unsatisfactory, so a further experimental clarification is due. We think that in understanding of the $^5$H system we have come to a position, when to improve things we need highly detailed information: precise invariant-mass data in a broad energy range. From the theoretical point of view it is very important that correlation spectra of the particles from $^5$H decay become available; we have shown above and in the paper [1] that they make interpretation of the data much more unambiguous.

The optimal experiment to resolve the existing experimental puzzle could be one combining feature of the experiments [2,4]. For example, proton knockout on a proton target, but at a larger energy than in [2].

Numerous useful discussions with people involved in the experimental search for $^5$H are acknowledged. I should mentioned here L. Chulkov, M. Golovkov, B. Jonson, A.A. Korsheninnikov, M. Meister, Yu.Ts. Oganessian, H. Simon and G.M. Ter-Akopian. The author is thankful to B. Danilin, N. Shulgina, and M. Zhukov for discussions on the theoretical aspects of the problem and to H. Simon and L. Chulkov for careful reading of the manuscript. The author acknowledges the financial support from the Royal Swedish Academy of Science. The work was partly supported by the RFBR grants 00-15-96590 and 02-02-16174.

## References

1. L.V. Grigorenko, N.K. Timofeyuk, M.V. Zhukov, Eur. Phys. J. A **19**, 181 (2004).
2. A.A. Korsheninnikov *et al.*, Phys. Rev. Lett. **87**, 092501 (2001).
3. M. Golovkov *et al.*, Phys. Lett. B **566**, 70 (2003).
4. M. Meister *et al.*, Nucl. Phys. A **723**, 13 (2003); Phys. Rev. Lett. **91**, 162504 (2003).
5. G.F. Filippov, A.D. Bazarov, K. Kato, Yad. Fiz. **62**, 1763 (1999) (Phys. At. Nucl. **62**, 1642 (1999)).
6. N.B. Shul'gina, B.V. Danilin, L.V. Grigorenko, M.V. Zhukov, J.M. Bang, Phys. Rev. C **62**, 014312 (2000).
7. P. Descouvemont, A. Kharbach, Phys. Rev. C **63**, 027001 (2001).
8. N.K. Timofeyuk, Phys. Rev. C **65**, 064306 (2002).
9. E.G. Adelberger *et al.*, Phys. Lett. B **25**, 595 (1967).
10. P.G. Young, R.H. Stokes, G.G. Ohlsen, Phys. Rev. **173**, 949 (1968).
11. R.B. Weisenmiller *et al.*, Nucl. Phys. A **280**, 217 (1977).
12. A.V. Belozerov *et al.*, Nucl. Phys. A **460**, 352 (1986).
13. M.G. Gornov *et al.*, Pis'ma Zh. Eksp. Teor. Fiz. **45**, 205 (1987), (JETP Lett. **45**, 252 (1987)).
14. M.G. Gornov *et al.*, Nucl. Phys. A **531**, 613 (1991).
15. K. Seth, B. Parker, Phys. Rev. Lett. **66**, 2448 (1991).
16. D.V. Aleksandrov, E.Yu. Nikolsky, B.G. Novatsky, D.N. Stepanov, in *Proceedings of the International Conference on Exotic Nuclei and Atomic Masses, Arles, France, June 19-23, 1995*, edited by M. de Saint Simon, O. Sorlin (Editions Frontieres, Gif-sur-Yvette, 1995) p. 329.
17. A.A. Korsheninnikov, E.Yu. Nikolsky, A.A. Ogloblin, Pis'ma Zh. Eksp. Teor. Fiz. **46**, 306 (1987), (JETP Lett. **46**, 384 (1987)).
18. M.G. Gornov *et al.*, Pis'ma Zh. Eksp. Teor. Fiz. **77**, 412 (2003).
19. L.V. Grigorenko, B.V. Danilin, V.D. Efros, N.B. Shul'gina, M.V. Zhukov, Phys. Rev. C **57**, R2099 (1998).
20. L.V. Grigorenko, B.V. Danilin, V.D. Efros, N.B. Shul'gina, M.V. Zhukov, Phys. Rev. C **60**, 044312 (1999).
21. M.V. Zhukov, B.V. Danilin, D.V. Fedorov, J.M. Bang, I.J. Thompson, J.S. Vaagen, Phys. Rep. **231**, 151 (1993).
22. L.M. Delves, Nucl. Phys. **20**, 275 (1960).
23. B.V. Danilin *et al.*, Yad. Fiz. **46**, 427 (1987), (Sov. J. Nucl. Phys. **46**, 225 (1987)).
24. O.V. Bochkarev *et al.*, Pis'ma Zh. Eksp. Teor. Fiz. **40**, 204 (1984), (JETP. Lett. **40**, 969 (1984)).
25. O.V. Bochkarev *et al.*, Pis'ma Zh. Eksp. Teor. Fiz. **42**, 303 (1985), (JETP. Lett. **42**, 374 (1985)).
26. O.V. Bochkarev *et al.*, Nucl. Phys. **A505**, 215 (1989).

27. O.V. Bochkarev *et al.*, Yad. Fiz. **49**, 1521 (1989), (Sov. J. Nucl. Phys. **49**, 941 (1989)).
28. O.V. Bochkarev *et al.*, Yad. Fiz. **55**, 1729 (1992), (Sov. J. Nucl. Phys. **55**, 955 (1992)).
29. O.V. Bochkarev *et al.*, Yad. Fiz. **57**, 5 (1994), (Sov. J. Nucl. Phys. **57**, 1281 (1994)).
30. O.V. Bochkarev *et al.*, Yad. Fiz. **52**, 1525 (1990), (Sov. J. Nucl. Phys. **52**, 964 (1990)).
31. L.V. Grigorenko, M.V. Zhukov, Phys. Rev. C **68**, 054005 (2003).
32. L.V. Grigorenko, I.G. Mukha, M.V. Zhukov, Phys. Rev. Lett. **88**, 042502 (2002).
33. L.V. Grigorenko, R.C. Johnson, I.G. Mukha, I.J. Thompson, M.V. Zhukov, Eur. Phys. J. A **15**, 125 (2002).